DE VITO: A Dual-arm, High Degree-of-freedom, Lightweight, Inexpensive, Passive Upper-limb Exoskeleton for Robot Teleoperation

Fabian Falck*, Kawin Larppichet*, and Petar Kormushev

Robot Intelligence Lab, Dyson School of Design Engineering,
Imperial College London, UK
https://www.imperial.ac.uk/robot-intelligence/
{fabian.falck17, kawin.larppichet17, p.kormushev}@imperial.ac.uk

Abstract. While robotics has made significant advances in perception, planning and control in recent decades, the vast majority of tasks easily completed by a human, especially acting in dynamic, unstructured environments, are far from being autonomously performed by a robot. Teleoperation, remotely controlling a slave robot by a human operator, can be a realistic, complementary transition solution that uses the motion intelligence of a human in complex tasks while exploiting the robot's autonomous reliability and precision in less challenging situations.
We introduce DE VITO, a seven degree-of-freedom, dual-arm upper-limb exoskeleton that passively measures the pose of a human arm. DE VITO is a lightweight, simplistic and energy-efficient design with a total material cost of at least an order of magnitude less than previous work. Given the estimated human pose, we implement both joint and Cartesian space kinematic control algorithms and present qualitative experimental results on various complex manipulation tasks teleoperating Robot DE NIRO, a research platform for mobile manipulation, that demonstrate the functionality of DE VITO. We provide the CAD models, open-source code and supplementary videos of DE VITO at http://www.imperial.ac.uk/robot-intelligence/robots/de_vito/.

Keywords: Upper-limb exoskeleton · Teleoperation · Remote control · Semi-autonomous control · Human-in-the-loop control · Manipulation

1 Introduction

Robots have proven to reliably outperform humans on low-variability, repetitive tasks which guarantee constraints suiting an autonomous operation. However, in spite of rapid advances in robotics in recent decades, robots cannot autonomously handle the vast majority of typical human tasks acting in unstructured, dynamic environments where plans and motions cannot be easily derived by a machine

* Equal contribution.

Fig. 1: CAD model of the DE VITO, an upper-limb exoskeleton consisting of two arms and the electronics body.

[7]. For instance, in the DARPA Robotics Challenge, robots have to complete a course in almost full autonomy and solve tasks, such as driving and egressing a vehicle, opening a door and a valve, drilling or climbing stairs [2]. In spite of the highly predefined, static environment, the competition illustrated the limitations of robots in such settings which are easily solvable by a human. To give a second example, in the context of social assistance robotics, especially manipulation tasks can have a challenging nature due to their high task complexity and variability introduced by interacting humans [6]. Both examples show that while robots are in principle equipped with super-human sensor (e.g. 3D LIDAR, 360-degree vision) and actuator (e.g. AC servo motor, hydraulic motor) hardware, their capabilities lack the cognitive capabilities of making sense of these inputs and produce flexible actions. This is why robots operating in non-predefined, complex environments had little to no impact on our everyday lives up until now. Therefore, we argue that *teleoperation*, controlling a robot remotely (i.e. at a physical distance) by a human operator, can be an approach to utilize the motion intelligence and creativity of a human for such tasks while exploiting the robot's autonomous reliability and repetitive precision in all other situations. Such a human-in-the-loop, semi-autonomous operation can be an important and realistic complementary approach to integrate robots effectively and act as a transition solution in the years ahead [11].

While various human-robot interfaces exist to control a robot, this work proposes an upper-limb exoskeleton we call *DE VITO (Design Engineering's Virtual Interface for TeleOperation)*. Fig. 1 shows the rendered CAD model of DE VITO. The exoskeleton passively measures the state of a human arm (master) with its seven degrees of freedom. This in turn controls a slave robot through a kinematic mapping procedure. In designing DE VITO, we aim at and achieve the following five design goals for our system: (1) A *few-component, high degree-of-freedom (DOF)*, *dual-arm* design, without sacrificing in measurement precision on manipulation tasks and in comparison to previous designs that have a small number of DOFs (2) *Passive* measurement with minimal impact on the human operator (3) A *lightweight and wearable* and therefore portable suite directly mounted on the operator (4) *Low-energy*, highly optimized electronic components (5) An *inexpensive* design with an estimated total material cost of at

least an order of magnitude less than previous work which is crucial to make the exoskeleton design more widely accessible. Potential applications of DE VITO are, for example, as a teaching interface in imitation learning, as an interface in dual-arm coordination experiments, as a virtual reality control interface, or as a teleoperation interface in hazardous or highly complex enviroments (e.g. social assistance robotics).

The main contributions of this work are as follows: 1) A discussion of state-of-the-art upper-limb exoskeleton literature, examining their design characteristics 2) the mechanical and electronic design of DE VITO and a comparison of three kinematic control procedures 3) qualitative experiments that demonstrate DE VITO's functionality on Robot DE NIRO [6], a mobile manipulation research platform, in several complex manipulation tasks.

The remainder of this work is organized as follows: In section 2, we discuss the related work. In section 3, we derive and explain technical details of the design of DE VITO. In section 4, we discuss our experiments with DE VITO on Robot DE NIRO and conclude our work in section 5.

2 Related Work

In this section, we discuss prior work on controlling a robot arm system through a human-operated, teleoperation method or device during manipulation. In a review by Field et al., the authors classify motion capturing methods into four categories: 1) optical, through computer vision systems that capture the human pose either with passive or active markers or markerless 2) inertial, by measuring acceleration and rotational velocities with triaxial accelerometers and gyroscopes 3) magnetic, by measuring electromagnetic fields caused from mounted transmitters and 4) mechanical, by directly measuring the joint angles through potentiometers. In this work and while discussing related approaches during this section, we focus on a *mechanical* exoskeleton design to capture the motion of a human arm for the following reasons: First, while an optical system can provide highly accurate pose estimates, the fastest real-time, analog convolution operations have a frame rate of 166 Hz (upper-bound estimate, since frame rate would drop in multilayer architecture) [5]. This would introduce a significant latency into the control loop. Furthermore, a user would have to actively avoid visual occlusion relative to one or multiple cameras. Second, while inertia sensors can capture a large range of motion, they lack the accuracy and also the sampling frequency required for a reactive teleoperation system. Third, a mechanical design is inexpensive, lightweight and can easily provide sampling rates of about 1 kHz. In addition, a mechanical exoskeleton could feed a physical interaction with the environment back to the user, a crucial feature for controlling the robot on manipulation tasks in the real world [9].

Various reviews have discussed the current state-of-the-art of mechanical exoskeletons [8]. A first key design challenge is the shoulder joint of the exoskeleton. With regards to the kinematics of the exoskeleton, it is problematic that the human arm's centre of rotation is changing during the motion as this causes a

small misalignment of the rotation axis. One way to overcome this issue is by preventing and compensating the misalignment through an internally exerted force onto the human arm [10]. The majority of designs, however, estimate the arm pose with a passive approach, as this allows a more natural, user-friendly interaction. To prevent the rotational centre from moving in passive designs, the shoulder joint (compare section 3.1), consisting of a ball and socket joint, is often imitated by three connected revolute joints. However, this technically simple solution comes at the cost a potential gimbal lock, if two rotational axes are colinear or lay within the same plane. If gimbal lock applies, the exoskeleton's degree of freedom is reduced by one. Considering this additional singularity point, previous work proposed to, for example, place the shoulder joint at enough distance from the operator such that the singularity cannot be reached within the workspace of the robot [15], or introduced additional, redundant degrees of freedom to the exoskeleton [14]. For our design, we propose a passive measurement with the shoulder joint being very close to the operator, making the design compact and wearable, while placing the singularity point in a favorable (because not important during operation) pose of the exoskeleton.

Moreover, we want to highlight three particularly promising mechanisms to measure internal rotation and briefly discuss the differences to our design, all illustrated in Fig. 2. Perry et al. propose a semi-circular bearing design which isolates each joint (no interacting joint measurements in one-dimensional rotations) allowing a precise, isolated measurement [16]. However, this design is both heavy ($\approx$ 10 kg in total) and expensive. In comparison, the Toyota T-HR3 Master Maneuvering System is linked by four bars and therefore requires at least four revolute joints and numerous moving parts to operate, making its design overly complicated [1]. Kim et al. propose a design with non-90-degree linkage of rotation axes, which is based on only three revolute joints (like ours). However, in any arm motion, multiple joints are involved in the measurement process, overcomplicating the procedure [12]. In comparison, our design aims at a simplistic (few moving parts), lightweight and inexpensive (one single joint with an encoder used in [16] [1] [12] has a cost higher than the total material cost of our work) design without sacrificing in measurement precision.

3 Design and Implementation

3.1 Human arm motion

The purpose of DE VITO is to estimate the pose of a human arm by measuring its joint angles. In order to understand possible motions of a master operator, we first review the simple arm model (ignoring minor misalignment due to human joint translation) in human kinesiology. The human arm consists of seven degrees of freedom, illustrated in Fig. 3: Three rotations at the glenohumeral (shoulder) joint (1-3), one rotation at the elbow joint (4), one rotation at the radioulnar joint on the forearm (5) and two rotations at the wrist joint (6-7). The Range of Motion (RoM) is defined as the maximum span of a human arm in positive and negative direction with regards to a given reference frame. It was empirically

Fig. 2: Comparison of internal rotation measurement approaches. Semi-circular bearing design (top left) [16], four-bar linkage design (top right) [1], three non-90-degree linkage design (bottom left) [12], our offset linkage design (bottom right).

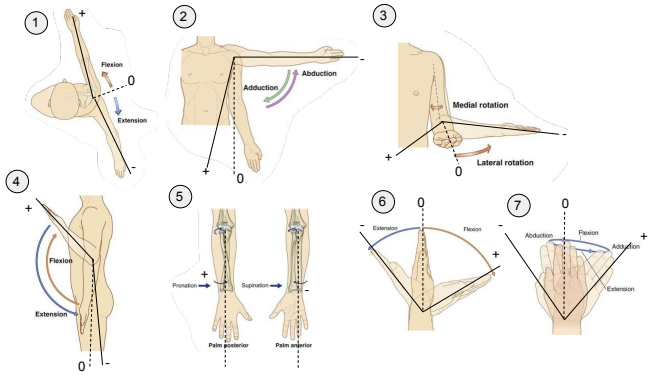

Fig. 3: Degrees of freedom of a human arm. 1-3: Glenohumeral joint, 4: Elbow joint, 5: Radioulnar joint, 6-7: Wrist joint. The thin black lines indicate the positive and negative range and the null reference. Figures adapted from [4].

studied by Boone et al. on a set of human male subjects [3] and is listed together with the covered range of motion of our exoskeleton design in Table 1.

3.2 Mechanical design

We explain the mechanical design of DE VITO by first discussing the upper part (shoulder joint), then the lower part (wrist joint and end-effector control).

As discussed in section 2, the placement of the shoulder joint in an upper-limb exoskeleton is difficult, due to the moving rotational centre in a human arm, and important, as gimbal lock can reduce the degrees of freedom of the exoskeleton. While the singularity point cannot be avoided, the exoskeleton can be designed in such a way that gimbal lock occurs either outside of the workspace of the robot (compare [15]) or at least in an operationally less important pose.

Fig. 4 compares the CAD models of three design variants (A to C) for the right arm differing in the placement of the shoulder joint, also known as singularity placement. All CAD models were designed using Fusion 360. In all

Table 1: Comparison of the Range of Motion (RoM) between a human arm [3] and our proposed exoskeleton design. The first value of RoM represents maximum positive, the second maximum negative span in degrees with regards to the given reference frame in Fig. 3.

Anatomic part	Joint description and type	Motion description	Human arm RoM [deg.]	Exoskeleton RoM [deg.]	Coverage percentage [%]
Shoulder	Glenohumeral joint (ball and socket joint)	Flexion/Extension	(158,53)	(110,55)	78
		Adduction/Abduction	(0,170)	(0,110)	64
		Medial/Lateral rotation	(70,90)	(110,110)	100
Elbow	Elbow joint (hinge joint)	Flexion/Extension	(146,0)	(110,110)	75
Forearm	Radioulnar joint (pivot joint)	Pronation/Supination	(71,84)	(110,110)	100
Wrist	Wrist joint (saddle joint)	Flexion/Extension	(73,71)	(110,55)	88
		Adduction/Abduction	(33,19)	(25,180)	100

three renderings, the camera pose is the same with gravity pointing downwards. The green arrows indicate rotational degrees of freedom. The three variants are shown in the pose of their kinematic singularity, occurring when the rotational axis along the upper-arm linkage (joint 3) is colinear with the first rotational axis at the the shoulder joint (joint 1). The red arrows indicate the rotational direction of this kinematic singularity. In variant A, gimbal lock occurs when both arm linkages point fowards and are colinear with the sagittal axis and removes the rotational degree of freedom within the transverse plane, which is highly unfavourable as it lies in the most used workspace area of a robot. In variant B, gimbal lock occurs when both arm linkages point outwards being colinear with the frontal axis, prohibiting a rotational movement in the transverse plane. While this pose is infrequent during normal operation, it can be relevant to specific manipulation tasks, such as picking up an object and placing it in a box on the side of the robot. In variant C, gimbal lock occurs in the "relaxed pose" when both arm linkages point downwards, being colinear with the longitudinal axis and prohibiting rotational movement in the frontal plane. This singularity pose is by far the most favorable for two reasons: First, operation is unlikely in this pose. Second, it is outside of the workspace of most upper-body manipulation robots, such as the Baxter arms of DE NIRO which we use in the experimental section. Therefore, we chose variant C for our final design.

The lower part of the exoskeleton is illustrated in Fig. 6. It was designed in such a way that the forearm rotational axis (pronation/supination; blue dashed line) is perpendicular with the pitch and yaw axis of the controller (purple dashed lines) which allows a comfortable and ergonomic motion to rotate the end-effector. On top of the first joint, we mount a Nunchuk controller typically used as a controller for a Nintendo Wii game console. The Nunchuk's two buttons are mapped to open and close a gripper and, in the case of an emergency, to immediately disable teleoperation (Baxter arms remain on last published coordinates) in accordance with the industrial robot ISO 10218. The small joystick, which is controllable by the thumb, is used for fine manipulation movements in the transverse plane.

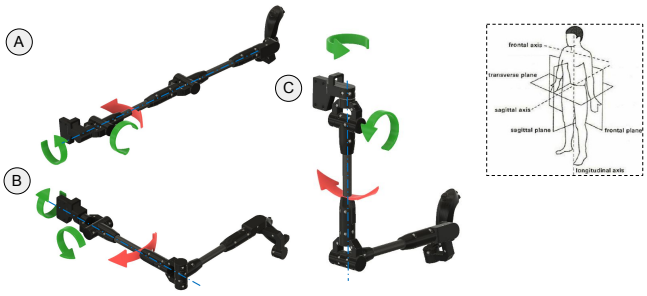

Fig. 4: CAD models of three design variants (right arm only) for the shoulder joint. The green arrows indicate rotational degrees of freedom, the red arrows indicate the rotational direction of kinematic singularity, if the rotational axis along the upper arm linkage is colinear with the last rotational axis at the shoulder joint. Variant C is chosen as our final design. Source of right-hand image: [13].

The complete mechanical design (CAD model and kinematic diagram) is illustrated in Fig. 5. As before, the green arrows indicate the seven rotational degrees of freedom of the design. Its corresponding Denavit-Hartenberg (DH) parameters are listed in Table 2. The total weight of the design is 3.2 kg (including the central electronics board), with each arm contributing 0.85 kg. This fulfills our initial goal of a lightweight, portable design that can be easily carried for prolonged amounts of time in operation mode. With regards to manufacturing DE VITO, all seven joints were 3D printed from ABS+, particularly suited for robust designs and good at avoiding warping. For manufacturing the links, we use carbon fiber fishing rod with a diameter of approximately 18 mm.

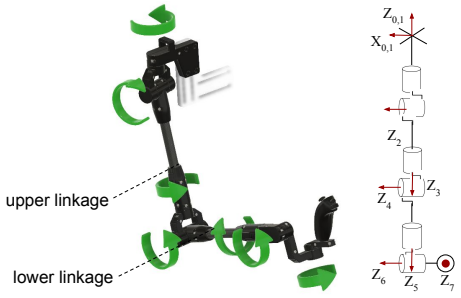

Fig. 5: CAD model of one arm of DE VITO (without central body) and its corresponding kinematic diagram. The green arrows represent the seven degrees of freedom of the arm. The brown arrows represent the seven Z and the X vectors in DH notation. Note that all other X and Y vectors follow from the right-hand rule and the initial coordinate frame.

Index i	a_i	α_i	d_i	θ_i
1	0	0	0	θ_1
2	0	$\frac{\pi}{2}$	0	θ_2
3	0	$\frac{\pi}{2}$	0.37	θ_3
4	0	$-\frac{\pi}{2}$	0	θ_4
5	0	$\frac{\pi}{2}$	0.33	θ_5
6	0	$-\frac{\pi}{2}$	−0.07	θ_6
7	0	$\frac{\pi}{2}$	−0.07	θ_7

Table 2: DH table of DE VITO. a_i represents the length of the common normal of joint axes i and $(i-1)$, α_i represents the angle between two adjacent joint axes, and d_i represents the offset along Z_{i-1} to the common normal.

The electronic components of the exoskeleton mainly comprises one Arduino mega, one MPU6050 breakout, one I2C multiplexer, two terminal blocks, and potentiometers described below. All components except for the potentiometers are mounted on a central circuit body covered in a plastic frame and worn on the

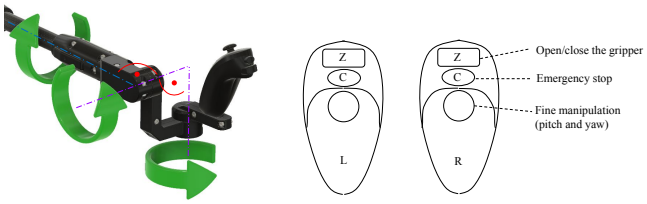

Fig. 6: CAD model of the lower part of DE VITO (left) and Nunchuk interface to control an end-effector (right). The green arrows indicate the rotational degrees of freedom.

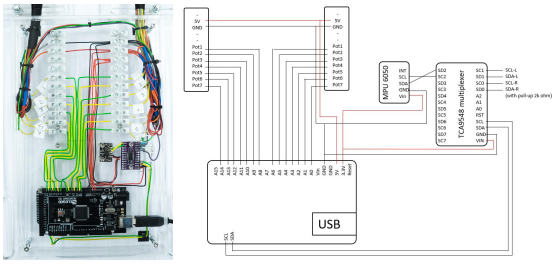

Fig. 7: Circuit board body (left), and corresponding wiring diagram (right) of DE VITO. The circuit board's main components are one Arduino mega, one I2C multiplexer, one MPU6050 breakout, and two terminal blocks.

back of the operator. A program running on the Arduino mega reads all sensor measurements and forwards them to a ROS node to compute the forward and inverse kinematics, as explained in section 3.3. In order to use this very inexpensive and energy-efficient micro controller, we conducted a low-level hardware and code optimization by 1) parallelizing potentiometer measurements with an interrupt handle 2) increasing the clock speed of the Arduino mega to the maximum, yet stable value 3) adjusting the encryption and minimizing the number of bytes during serial communication from 63 to 23 bytes per reading sample. Doing so, we achieve an effective sampling rate of the serial communication of 720 Hz, a ten-times increase compared to before the optimization, which is sufficient for reactive, precise feedback for the manipulation tasks in section 4.
The MPU6050 is functioning as an IMU sensor. It allows to measure the yaw of the operator (rotation around the longitudinal axis) and therefore enables, if required, the slave-robot to turn on the spot. The I2C multiplexer is required to communicate with multiple same-address devices and furthermore allows extending DE VITO with additional sensors in future work. The circuit board body together with its corresponding wiring diagram is illustrated in Fig. 7.

In order to measure the joint angles, we use seven rotary potentiometers per arm, omitting expensive encoders in the related work, with an electrical angle of rotation of 260 degrees, being sufficient to cover the range of motion of all exoskeleton joints. Due to the limitation of the Arduino mega to 10 bits per analog signal, the resolution of the potentiometers is limited to $\frac{260 \text{ deg.}}{2^{10}} \approx 0.25$ degree. In

our experiments, we found this sensitivity to be more than sufficient for smooth, precise teleoperation by a human.

The approximate total material cost of the design is 200 GBP, including 3D printing materials ($\approx$ 70 GBP), carbon tubes and mechanical parts ($\approx$ 60 GBP) and electronic parts ($\approx$ 70 GBP), making our design at least an order of magnitude less expensive than prior exoskeleton designs discussed in section 2.

3.3 Kinematic Control algorithm and Calibration

In the following, we define the kinematic mapping procedures from the exoskeleton pose to the robot pose which we further explore in the experimental section. In the following, θ_i^{master} and θ_i^{slave} refer to the i-th joint angle of the master (exoskeleton) and the slave (e.g. Robot DE NIRO), respectively.

(1) *Joint space one-to-one*: The simplest way to align the two spaces spaces is by mapping each angle one-to-one as follows:
$\theta_i^{slave} = \theta_i^{master} + \theta_i^{offset}$, where θ_i^{offset} is an offset angle of joint i that accounts for the difference in the null reference in both spaces. From the operator's perspective, this control procedure is most intuitive, as, for example, a rotation of the i-th exoskeleton joint by an angle β directly results in a rotation of the i-th robot arm joint by β. However, it comes at the disadvantage that the range of motion of the master operator (human) limits the range of motion of the slave (robot), although the latter is typically larger.

(2) *Joint space scaled*: To overcome this shortcoming, we use joint-specific factors c_i that linearly scale the mapping as follows:
$\theta_i^{slave} = c_i * \theta_i^{master} + \theta_i^{offset}$. By upscaling the master angles, the operator can access a larger range of motion of the slave robot. However, controlling the slave robot this way is less intuitive and is therefore subject to experiments.

(3) *Cartesian space*: In addition to the joint space control procedures, we provide a more high-level, Cartesian control approach controlling the end-effector pose of the slave robot $P^{\text{slave}}_{\text{end-effector}}$, given the pose of the exoskeleton's end-effector $P^{\text{master}}_{\text{end-effector}}$. The control procedure consists of three steps: First, we calculate the slave's end-effector pose (6 DOFs) as follows: $P^{\text{slave}}_{\text{end-effector}} = P^{\text{master}}_{\text{end-effector}} + d_{\text{offset}}$, where d_{offset} is an offset pose to guarantee operation in the slave robot's workspace. This remains one DOF undefined (nullspace), which is why we impose a constraint on the elbow joint, fixing it in a specific rotation. Fig. 8 illustrates two different elbow joint constraints which can be switched between by the user depending on the exact manipulation task at hand. Third, we use Robot DE NIRO's inverse kinematics solver to compute the joint angles and actuate accordingly.

4 Experiments

In the following, we describe our qualitative experiments and results that demonstrate DE VITO's general functionality. The experiments apply the exoskeleton to teleoperate in complex manipulation tasks which would require – if at all

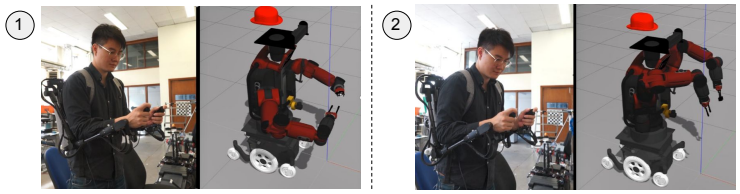

Fig. 8: Comparison of two imposed elbow constraints (1 and 2) under Cartesian space control. Note that while the human pose is approximately identical (left), the robot pose differs depending on the elbow constraint (right).

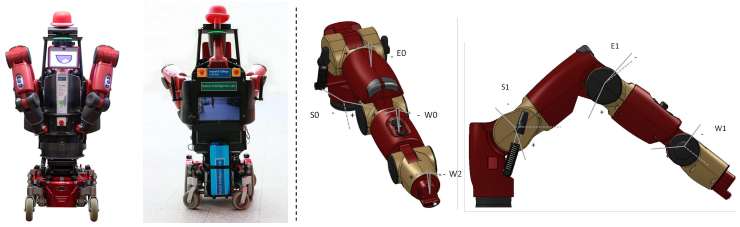

Fig. 9: Left: Robot DE NIRO [6], a research platform for mobile manipulation, used as the experimental slave robot of this work, right: Baxter arms for manipulation and their seven degrees-of-freedom at shoulder (S), elbow (E) and wrist (W). Source of figures on right-hand side: [17].

explored by current literature – a computationally costly training procedure to perform them autonomously.

4.1 Experimental platform

As the experimental platform and slave-robot for our experiments, we use Robot DE NIRO [6], a research platform for mobile manipulation, and integrated the communication of both systems via the Robot Operating System (ROS). DE NIRO is a humanoid robot with Baxter dual-arms mounted on top of a QUICKIE electric wheelchair base. The Baxter arms have seven degrees of freedom each and are mainly made of twist and bend joints. The control loop cycle frequency of the Baxter arms, including receiving an asynchronous message and execution, is 1 kHz, therefore not limiting the exoskeleton control effectively sampled at a frequency of 720 Hz [17]. For our experiments, we will not make use of DE NIRO's navigation capabilities and will only operate the robot in stationary mode. Furthermore, DE NIRO is equipped with a large amount of sensors, including a Microsoft Kinect RGB-D camera, a 360-degree camera rig, ultrasonic and infrared proximity sensors and 2D and 3D LIDARs. DE NIRO together with two functional views of its Baxter arms is illustrated in Fig. 9. In addition, we optionally use an HTC Vive as an immersive interface for the user that displays the Kinect sensor data and allows controlling DE NIRO in virtual reality.

Fig. 10: Qualitative manipulation experiments with Robot DE NIRO as the slave robot: Grasping a cup and handing it over (top left), brick stacking (top right), grasping a bottle (bottom left), and a peg-in-hole task with allen keys (bottom right).

4.2 Teleoperated manipulation tasks and Results

We tested the functionality of the exoskeleton qualitatively on four manipulation tasks, illustrated in Fig. 10: Grasping and handing over cups and bottles, stacking bricks and a peg-in-hole task. We drew three key insights from these experiments: First, all manipulation tasks could be completed by untrained human subjects teleoperating Robot DE NIRO, demonstrating the general functionality of DE VITO. Second, we found that the scaled control procedure described in section 3.3 can be easily learned by a human and empirically fine-tuned the scaling factors c_1 to c_7 as $\{1.0, 1.2, 1.5, 1.0, 1.3, 1.5, 1.5\}$, considering the trade-off between a larger effective range of motion of the robot (what the exoskeleton actually maps to) with the effective precision of the exoskeleton (too large scaling factors cause a overly reactive procedure). Third, we found the Cartesian space control to be most intuitive and easy to use for subjects, as their visual feedback can be focussed on the end-effector pose.

5 Conclusion

In this work, we introduced DE VITO, a dual-arm, passive, wearable, and simplistic upper-limb exoskeleton to teleoperate robots in complex manipulation tasks and demonstrated its general functionality in qualitative experiments. DE VITO's design has several limitations: There is no haptic feedback on the exerted force, e.g. in the form of touch, to the user, making tasks such as grasping soft or elastic objects difficult. In addition, although the precision of the manipulation actions through DE VITO is remarkable given its inexpensive, low-energy and light-weight design, further research and experiments are required to evaluate the degree to which general manipulation tasks are solvable with the exoskeleton. We will in addition integrate DE VITO with Robot DE NIRO to experiment with a semi-autonomous, combined use case for manipulation.

References

1. Ackerman, E.: Toyota Gets Back Into Humanoid Robots With New T-HR3. https://spectrum.ieee.org/automaton/robotics/humanoids/toyota-gets-back-into-humanoid-robots-with-new-thr3 (2018)
2. Ackerman, E., Guizzo, E.: DARPA Robotics Challenge Finals: Rules and Course. https://spectrum.ieee.org/automaton/robotics/humanoids/drc-finals-course (2018)
3. Boone, D.C., Azen, S.P.: Normal range of motion of joints in male subjects. The Journal of Bone and Joint Surgery **61**(5), 756–759 (1979)
4. clinicalgate.com: Upper Limb - General description. https://clinicalgate.com/upper-limb-2/ (2015)
5. Debrunner, T., Saeedi, S., Kelly, P.H.: Auke: Automatic kernel code generation for an analogue simd focal-plane sensor-processor array. ACM Transactions on Architecture and Code Optimization (TACO) **15**(4), 59 (2019)
6. Falck, F., Doshi, S., Smuts, N., Lingi, J., Rants, K., Kormushev, P.: Human-centered manipulation and navigation with Robot DE NIRO. In: Intelligent Robots and Systems (IROS) Workshop Towards Robots that Exhibit Manipulation Intelligence, 2018 IEEE/RSJ International Conference on. (2018)
7. Fang, B., Guo, D., Sun, F., Liu, H., Wu, Y.: A robotic hand-arm teleoperation system using human arm/hand with a novel data glove. In: Robotics and Biomimetics (ROBIO), 2015 IEEE International Conference on. pp. 2483–2488. IEEE (2015)
8. Gopura, R., Kiguchi, K., Bandara, D.: A brief review on upper extremity robotic exoskeleton systems. In: Industrial and Information Systems (ICIIS), 2011 6th IEEE International Conference on. pp. 346–351. IEEE (2011)
9. Hirche, S., Buss, M.: Human-oriented control for haptic teleoperation. Proceedings of the IEEE **100**(3), 623–647 (2012)
10. Jarrasse, N., Morel, G.: Connecting a human limb to an exoskeleton. IEEE Transactions on Robotics **28**(3), 697–709 (2012)
11. Kemp, C.C., Edsinger, A., Torres-Jara, E.: Challenges for robot manipulation in human environments [grand challenges of robotics]. IEEE Robotics & Automation Magazine **14**(1), 20–29 (2007)
12. Kim, B., Deshpande, A.D.: Controls for the shoulder mechanism of an upper-body exoskeleton for promoting scapulohumeral rhythm. In: Rehabilitation Robotics (ICORR), 2015 IEEE International Conference on. pp. 538–542. IEEE (2015)
13. Krishnan, R.H., Devanandh, V., Brahma, A.K., Pugazhenthi, S.: Estimation of mass moment of inertia of human body, when bending forward, for the design of a self-transfer robotic facility. J. Eng. Sci. Technol **11**(2), 166–176 (2016)
14. Lu, J., Haninger, K., Chen, W., Gowda, S., Tomizuka, M., Carmena, J.M.: Design of a passive upper limb exoskeleton for macaque monkeys. Journal of Dynamic Systems, Measurement, and Control **138**(11), 111011 (2016)
15. Nef, T., Mihelj, M., Kiefer, G., Perndl, C., Muller, R., Riener, R.: ARMin-Exoskeleton for arm therapy in stroke patients. In: Rehabilitation Robotics, 2007. ICORR 2007. IEEE 10th International Conference on. pp. 68–74. IEEE (2007)
16. Perry, J.C., Rosen, J., Burns, S.: Upper-limb powered exoskeleton design. IEEE/ASME transactions on mechatronics **12**(4), 408–417 (2007)
17. Robotics, R.: Baxter Research Robot SDK Wiki - Arm Control Overview and Hardware Specifications. http://sdk.rethinkrobotics.com/wiki/Arm_Control_Overview, http://sdk.rethinkrobotics.com/wiki/Hardware_Specifications (2015)